

Cascaded nonlinearity caused by local-field effects in the two-level atom

Ksenia Dolgaleva and Robert W. Boyd

The Institute of Optics, University of Rochester, Rochester, New York 14627, USA

John E. Sipe

Department of Physics, University of Toronto, Toronto, Ontario, Canada M5S 1A7

(Received 8 August 2007; published 12 December 2007)

Contributions to the fifth-order nonlinear optical susceptibility $\chi^{(5)}$ of a collection of homogeneously broadened two-level atoms that scale as $N^2(\gamma_{\text{at}}^{(3)})^2$ and $N^2|\gamma_{\text{at}}^{(3)}|^2$, where $\gamma_{\text{at}}^{(3)}$ is the lower-order atomic hyperpolarizability and N is the atomic number density, are predicted theoretically. These “cascaded” contributions are a consequence of local-field effects. We determine them from a fifth-order solution of the Lorentz-Maxwell-Bloch equations. They are missing from a straightforward generalization of Bloembergen’s result for the local field correction to the second order nonlinearity, but are recovered by a careful application of his general approach. We find that at high atomic densities ($N > 10^{15} \text{ cm}^{-3}$) the value of the cascaded third-order contribution can be as large as the “direct” fifth-order term in the expression for the fifth-order susceptibility.

DOI: 10.1103/PhysRevA.76.063806

PACS number(s): 42.65.An, 42.65.Hw, 32.80.Wr

I. INTRODUCTION

It is well known that the field driving an atomic transition in a material medium, the local field, is different in general from both the external field and the average field inside the medium. The difference from the average field does not play a significant role when one considers a low-density medium. To describe the optical properties of such a system, one can use the macroscopic (ensemble average) field in considering the Maxwell-Bloch equations. However, if the atomic density of a system exceeds $\approx 10^{15} \text{ cm}^{-3}$ [1], the influence of local-field effects becomes significant and cannot be neglected.

Local-field effects lead to a modification of the optical properties of dense media and, consequently, serve as a source of interesting new phenomena. For instance, steady-state solutions to the local-field-corrected Maxwell-Bloch equations indicate that it is possible to realize mirrorless optical bistability [2–5]. Also, an additional inversion-dependent frequency shift appears. This frequency shift, called the Lorentz redshift, was experimentally measured in the reflection spectrum of a dense alkali-metal vapor [6,7]. The Lorentz redshift can cause a pulse to acquire a dynamic chirp, which enables soliton formation at a very low level of atomic excitation [8,9]. In a collection of three-level atoms, local-field effects can lead to inversionless gain and the enhancement of the absorptionless refractive index by more than two orders of magnitude [10–13]. Successful experimental attempts to realize this enhancement of the refractive index have been reported [14,15].

A phenomenological approach to treating local-field effects in nonlinear optics was proposed by Bloembergen [16]. He found that the local-field-corrected second-order nonlinear susceptibility scales as three powers of the local-field correction factor L , which is given in terms of dielectric permittivity $\epsilon^{(1)}$ for a uniform material as

$$L = \frac{\epsilon^{(1)} + 2}{3}. \quad (1)$$

The above expression is referred to as the Lorentz factor. It has been understood that Bloembergen’s result can be gener-

alized to a higher-order nonlinearity, and that the corresponding i th-order nonlinear susceptibility should scale as L^{i+1} (see, for example, Refs. [17,18]). In this paper we show theoretically that Bloembergen’s approach, when consistently applied, actually leads in fact to a much more complicated form for the nonlinear susceptibility. This is due to the presence of a cascading effect.

Cascading is a process in which a lower-order nonlinear susceptibility contributes to higher-order nonlinear effects in a multistep fashion; it has been a field of interest in nonlinear optics for some time. Macroscopic cascading has a nonlocal nature, in that the intermediate field generated by a lower-order nonlinearity propagates to contribute to a higher-order nonlinear process by nonlinearly interacting with the fundamental field [19–28]. Thus, it has been acknowledged that the experimentally measured third-order susceptibility can include contributions proportional to the square of the second-order susceptibility [19–21]. On the other hand, it has also been shown that nonlinear cascading is possible due to the local nature of the field acting on individual molecules in the medium [21,29–34]. This local-field-induced microscopic cascading does not require propagation and phase matching, and has a purely local character.

The fact that local-field effects create cascaded contributions of the lowest order hyperpolarizability $\gamma_{\text{at}}^{(2)}$ to the third-order susceptibility was first demonstrated by Bedeaux and Bloembergen [29]. They presented a general relationship between macroscopic and microscopic nonlinear dielectric response, obtained neglecting the pair correlation effect, which was later taken into account by Andrews *et al.* [33]. All the studies conducted thus far have concentrated on treating the local cascading contribution of $\gamma_{\text{at}}^{(2)}$ to third-order nonlinear effects, which only arises if the constituent molecules lack center of inversion symmetry.

We present a theoretical analysis of the nonlinear response of a two-level atom, treated up to the fifth order of nonlinearity, with local-field effects taken into account. In Sec. II, we address this problem by solving the local-field-corrected Maxwell-Bloch equations. We expand the total

susceptibility as a Taylor series in the electric field. We find that the resulting expression for the fifth-order nonlinear susceptibility is in disagreement with the straightforward generalization of Bloembergen's result [16] to fifth-order response. We resolve this apparent contradiction by solving the problem using a more careful implementation of Bloembergen's approach [29]. The detailed calculation shows that there is no disagreement between the results of the local-field-corrected Maxwell-Bloch equations and that careful implementation. Moreover, the results show that there is a cascaded contribution coming from the third-order microscopic hyperpolarizability, together with the naively expected fifth order nonlinear term. This cascaded contribution is a consequence of local-field effects.

In Sec. III we analyze the relative values of the contributions from the fifth- and third-order microscopic hyperpolarizabilities to $\chi^{(5)}$, and we find that under certain conditions the cascaded third-order contribution can be as large as the fifth-order contribution.

II. THEORETICAL APPROACHES

A. Maxwell-Bloch equations approach

A collection of two-level atoms with ground and excited states denoted, respectively, by a and b , interacting with an optical field closely tuned to an atomic resonance of the system, can be described by the Maxwell-Bloch equations [2,17]

$$\dot{\sigma} = \left(i\Delta - \frac{1}{T_2} \right) \sigma - \frac{1}{2} i\kappa E w \quad (2a)$$

and

$$\dot{w} = -\frac{w+1}{T_1} + i(\kappa E \sigma^* - \kappa^* E^* \sigma). \quad (2b)$$

Here $E(t)$ is the slowly varying amplitude of the macroscopic electric field $\tilde{E}(t) = E(t)\exp(-i\omega t) + \text{c.c.}$, and the total (linear and nonlinear) polarization $\tilde{P}(t) = P(t)\exp(-i\omega t) + \text{c.c.}$ involves

$$P(t) = N\mu^* \sigma(t), \quad (3)$$

where N is the number density of atoms, μ is the dipole transition moment of the two-level system from the ground to excited state, and $\sigma(t)$ is the slowly varying amplitude of coherence $\rho(t)$, that is,

$$\rho(t) = \sigma(t)\exp(-i\omega t). \quad (4)$$

In Eq. (2), $\kappa = 2\mu/\hbar$, $\Delta = \omega - \omega_{ba}$ is the detuning of the optical field frequency ω from the atomic resonance frequency ω_{ba} , T_1 and T_2 are, respectively, the population and coherence relaxation times, and w is the population inversion; we assume that the equilibrium value of w is $w_{\text{eq}} = -1$, corresponding to the ground state. According to the prescription of Lorentz [35], the field that appears in Eqs. (2) is actually the local field E_{loc} , which can be expressed in terms of the average field E and the polarization as

$$E_{\text{loc}} = E + \frac{4\pi}{3} P. \quad (5)$$

Expression (5) for the Lorentz local field can be substituted into the Maxwell-Bloch Eqs. (2) to yield

$$\dot{\sigma} = \left(i\Delta + i\Delta_L w - \frac{1}{T_2} \right) \sigma - \frac{1}{2} i\kappa w E \quad (6a)$$

and

$$\dot{w} = -\frac{w+1}{T_1} + i(\kappa E \sigma^* - \kappa^* E^* \sigma). \quad (6b)$$

The term $\Delta_L w$ entering the equation for σ introduces an inversion-dependent frequency shift, which is a consequence of local-field effects; the quantity Δ_L is called Lorentz red-shift and is given by

$$\Delta_L = -\frac{4\pi N |\mu|^2}{3 \hbar}. \quad (7)$$

The steady-state solutions to Eqs. (6) are

$$w = -\frac{1}{1 + \frac{|E|^2/|E_s^0|^2}{1 + T_2^2(\Delta + \Delta_L w)^2}} \quad (8a)$$

and

$$\sigma = \frac{\mu}{\hbar} \frac{wE}{\Delta + \Delta_L w + i/T_2}. \quad (8b)$$

In Eq. (8a) we introduced saturation field strength E_s^0 , defined as

$$|E_s^0|^2 = \frac{\hbar^2}{4T_1 T_2 |\mu|^2}. \quad (9)$$

As a consequence of the presence of the local-field-induced inversion-dependent frequency shift $\Delta_L w$ in Eq. (8a), the steady-state solution for the population inversion w becomes a cubic equation. In a certain range of parameters it has three real roots with absolute values not exceeding unity. The existence of three different physically meaningful solutions for the population inversion is associated with the phenomenon of local-field-induced optical bistability [2,4,5], first discussed by Hopf, Bowden, and Louisell [2]. In the appendix we identify the parameter space in which Eq. (8a) has multiple physical solutions, and show that it cannot be reached for the example system we consider later in this paper, the excitation of a collection of sodium atoms at frequencies close to the $3s \rightarrow 3p$ resonance.

For such systems, the nonlinear response can be studied through an approximate solution of Eq. (8a), obtained through a power-series expansion with respect to the electric field parameter $x = |E|^2/|E_s^0|^2$. Assuming x to be a small quantity, we perform a Taylor series expansion of w in terms of x ,

retaining only terms up to the second power, as we interested only in treating saturation effects up to the fifth order in E . The resultant solution for w takes the form

$$w = -1 + \frac{1}{1 + T_2^2(\Delta - \Delta_L)^2 |E_s^0|^2} \frac{|E|^2}{[1 + T_2^2(\Delta - \Delta_L)^2]^3} \frac{|E|^4}{|E_s^0|^4}. \quad (10)$$

The total polarization can be expressed in terms of the total susceptibility χ as $P = \chi E$. From Eq. (3), we find that

$$\chi = \frac{P}{E} = \frac{N\mu^* \sigma}{E}. \quad (11)$$

Substituting the steady-state solution for the coherence σ in the form (8b) into Eq. (11), we obtain

$$\begin{aligned} \chi &= \frac{N|\mu|^2 T_2}{\hbar} \frac{w}{T_2(\Delta + \Delta_L w) + i} \\ &= \frac{N|\mu|^2}{\hbar} \frac{(-w)}{[\omega_{ba} + \Delta_L(-w) - \omega] - i/T_2}. \end{aligned} \quad (12)$$

Equations (10) and (12) illustrate the physical effect of the nonlinearity: It is through the modification of the inversion parameter w from its equilibrium value of -1 , and that modification is twofold. First, the overall amplitude of the response is modified by the fact that $-w$ differs from unity, and second, the resonant frequency is modified from $\omega_{ba} + \Delta_L$ (the Lorentz-shifted low-intensity resonance frequency) to $\omega_{ba} + \Delta_L(-w)$.

It is convenient to represent the total susceptibility as a power series expansion with respect to the electric field:

$$\chi = \chi^{(1)} + 3\chi^{(3)}|E|^2 + 10\chi^{(5)}|E|^4 + \dots \quad (13)$$

Then, substituting the expansion of the population inversion (10) into Eq. (12) and making use of the representation (13) of the total susceptibility, we find the expressions for the linear and the nonlinear susceptibilities to be

$$\chi^{(1)} = -\frac{N|\mu|^2 T_2}{\hbar} \frac{T_2(\Delta - \Delta_L) - i}{1 + T_2^2(\Delta - \Delta_L)^2}, \quad (14a)$$

$$\chi^{(3)}|E_s^0|^2 = \frac{N|\mu|^2 T_2}{3\hbar} \frac{(T_2\Delta + i)[T_2(\Delta - \Delta_L) - i]^2}{[1 + T_2^2(\Delta - \Delta_L)^2]^3}, \quad (14b)$$

and

$$\chi^{(5)}|E_s^0|^4 = -\frac{N|\mu|^2 T_2}{10\hbar} \frac{(T_2\Delta + i)[1 - iT_2\Delta_L + T_2^2(\Delta - \Delta_L)(\Delta + 2\Delta_L)]}{[1 + T_2^2(\Delta - \Delta_L)^2]^3 [T_2(\Delta - \Delta_L) + i]^2}. \quad (14c)$$

B. The naive local-field correction

We next attempt to bring expressions (14) for the local-field-corrected susceptibilities to the form of Bloembergen's result. The straightforward generalization [17,18] of the Bloembergen's result to the case of the saturation effects [which are described by an odd-order nonlinearity as $\chi^{(i)} = \chi^{(i)}(\omega = \omega + \omega - \omega + \dots)$] reads

$$\chi^{(i)} = N\gamma_{\text{at}}^{(i)} |L|^{i-1} L^2, \quad (15)$$

where $\gamma_{\text{at}}^{(i)}$ is the i th-order microscopic hyperpolarizability.

Using Eqs. (2) and (4) for an isolated atom in free space, we write

$$\tilde{p}(t) = p \exp(-i\omega t) + \text{c.c.} \quad (16)$$

with

$$p = \mu^* \sigma \quad (17)$$

for the atom's dipole moment p . The Taylor series expansion for p with respect to the electric field yields

$$p = \gamma_{\text{at}}^{(1)} E + 3\gamma_{\text{at}}^{(3)} |E|^2 E + 10\gamma_{\text{at}}^{(5)} |E|^4 E + \dots \quad (18)$$

Here

$$\gamma_{\text{at}}^{(1)} = -\frac{|\mu|^2 T_2}{\hbar} \frac{T_2\Delta - i}{1 + T_2^2\Delta^2} \quad (19)$$

is the linear polarizability and

$$\gamma_{\text{at}}^{(3)} |E_s^0|^2 = \frac{|\mu|^2 T_2}{3\hbar} \frac{T_2\Delta - i}{(1 + T_2^2\Delta^2)^2} \quad (20a)$$

and

$$\gamma_{\text{at}}^{(5)} |E_s^0|^4 = -\frac{|\mu|^2 T_2}{10\hbar} \frac{T_2\Delta - i}{(1 + T_2^2\Delta^2)^3} \quad (20b)$$

are the third-order and fifth-order microscopic hyperpolarizabilities, respectively.

The definition of the factor L in terms of the dielectric function $\epsilon^{(1)}$ is given by Eq. (1). The next step is to find an expression for the factor L in terms of the detuning Δ and the

Lorentz redshift Δ_L . Setting $w=-1$ in Eq. (12), we arrive at

$$\chi^{(1)} = -\frac{N|\mu|^2 T_2}{\hbar} \frac{1}{T_2(\Delta - \Delta_L) + i}, \quad (21)$$

and so

$$\epsilon^{(1)} = 1 + 4\pi\chi^{(1)} = 1 - \frac{4\pi N|\mu|^2 T_2}{\hbar} \frac{1}{T_2(\Delta - \Delta_L) + i}. \quad (22)$$

Using Eq. (22) in Eq. (1), we obtain

$$L = \frac{T_2\Delta + i}{T_2(\Delta - \Delta_L) + i}. \quad (23)$$

Making use of Eq. (19) for microscopic polarizability, Eqs. (20) for microscopic hyperpolarizabilities, and Eq. (23) for factor L , we find that

$$N\gamma_{\text{at}}^{(1)}L = \chi^{(1)} \quad (24a)$$

of Eq. (14a),

$$N\gamma_{\text{at}}^{(3)}|L|^2L^2 = \chi^{(3)} \quad (24b)$$

of Eq. (14b), but

$$N\gamma_{\text{at}}^{(5)}|L|^4L^2 \neq \chi^{(5)} \quad (24c)$$

of Eq. (14c). In fact,

$$N\gamma_{\text{at}}^{(5)}|L|^4L^2 = \chi^{(5)} \frac{1 + T_2^2(\Delta - \Delta_L)^2}{1 - iT_2\Delta_L + T_2^2(\Delta - \Delta_L)(\Delta + 2\Delta_L)}. \quad (25)$$

Thus, the naive local-field correction (15) in terms of L 's is in disagreement with the correct result derived from the Maxwell-Bloch equations.

To find the origin of this disagreement, we address the problem of treating the saturation up to the fifth order of nonlinearity, following the recipe suggested by Bloembergen [16], rather than using the straightforward generalization given by Eq. (15). Our calculations are presented in the following subsection.

C. Bloembergen's approach

The polarization P entering Eq. (5) is the total polarization, given by the sum of the contributions proportional to first, third and fifth power of local electric field as

$$P = P^{(1)} + P^{(3)} + P^{(5)} + \dots \quad (26)$$

Here

$$P^{(1)} = N\gamma_{\text{at}}^{(1)}E_{\text{loc}}, \quad (27a)$$

$$P^{(3)} = N\gamma_{\text{at}}^{(3)}|E_{\text{loc}}|^2E_{\text{loc}}, \quad (27b)$$

and

$$P^{(5)} = N\gamma_{\text{at}}^{(5)}|E_{\text{loc}}|^4E_{\text{loc}}. \quad (27c)$$

Using Eq. (5) in Eq. (27a), we obtain

$$P^{(1)} = \frac{\epsilon^{(1)} - 1}{4\pi} \left[E + \frac{4\pi}{3}P^{(3)} + \frac{4\pi}{3}P^{(5)} + \dots \right]. \quad (28)$$

The electric displacement vector D is defined as

$$D = E + 4\pi P = E + 4\pi P^{(1)} + 4\pi P^{(3)} + 4\pi P^{(5)} + \dots \quad (29)$$

Substituting Eq. (28) into Eq. (29), we find that

$$D = \epsilon^{(1)}E + 4\pi P^{\text{NLS}}, \quad (30)$$

where

$$P^{\text{NLS}} = L(P^{(3)} + P^{(5)} + \dots) \quad (31)$$

is the nonlinear source polarization, introduced by Bloembergen [16].

Substituting expression (28) for the polarization $P^{(1)}$ into Eq. (26) for the total polarization, we find that

$$P = \chi^{(1)}E + P^{\text{NLS}}. \quad (32)$$

Substituting Eq. (5) for the local field into Eqs. (27b) and (27c) for the polarizations $P^{(3)}$ and $P^{(5)}$ and dropping out the terms scaling with higher than the fifth power of the electric field, we obtain

$$P^{(3)} = 3N\gamma_{\text{at}}^{(3)}|L|^2L|E|^2E + [24\pi N^2(\gamma_{\text{at}}^{(3)})^2|L|^4L^2 + 12\pi N^2|\gamma_{\text{at}}^{(3)}|^2|L|^6]E^4E \quad (33a)$$

and

$$P^{(5)} = 10N\gamma_{\text{at}}^{(5)}|L|^4L|E|^4E. \quad (33b)$$

Note that $P^{(3)}$ contains terms proportional to the fifth power of the electric field. Substituting Eq. (33) into Eq. (31), and Eq. (31) into Eq. (32), we find the total polarization to be

$$P = \chi^{(1)}E + 3N\gamma_{\text{at}}^{(3)}|L|^2L|E|^2E + [24\pi N^2(\gamma_{\text{at}}^{(3)})^2|L|^4L^3 + 12\pi N^2|\gamma_{\text{at}}^{(3)}|^2|L|^6L + 10N\gamma_{\text{at}}^{(5)}|L|^4L^2]E^4E + \dots \quad (34)$$

Alternatively, the total polarization can be represented as a Taylor series expansion with respect to the average electric field as

$$P = \chi E = \chi^{(1)}E + 3\chi^{(3)}|E|^2E + 10\chi^{(5)}|E|^4E + \dots \quad (35)$$

Equating (34) and (35), we obtain

$$\chi^{(1)} = N\gamma_{\text{at}}^{(1)}L, \quad (36a)$$

$$\chi^{(3)} = N\gamma_{\text{at}}^{(3)}|L|^2L^2, \quad (36b)$$

and

$$\chi^{(5)} = N\gamma_{\text{at}}^{(5)}|L|^4L^2 + \frac{24\pi}{10}N^2(\gamma_{\text{at}}^{(3)})^2|L|^4L^3 + \frac{12\pi}{10}N^2|\gamma_{\text{at}}^{(3)}|^2|L|^6L. \quad (36c)$$

Using expression (23) for the local-field correction factor, obtained in Sec. II C, one can show that Eqs. (36) for the local-field-corrected first, third, and fifth order susceptibilities are equivalent to Eqs. (14), obtained using the Maxwell-

Bloch approach. Thus, two different approaches—the Lorentz-Maxwell-Bloch equations and Bloembergen’s approach—bring us to the same result for the local-field-corrected susceptibilities. This is of course not surprising, since both approaches are just different ways of implementing Bloembergen’s scheme.

The expressions for local-field-corrected $\chi^{(1)}$ and $\chi^{(3)}$ do not display any peculiarity, while Eq. (36c) for $\chi^{(5)}$ deserves special attention. The first term on the right-hand side of the equation is due to a direct contribution from the fifth-order microscopic hyperpolarizability, while the two extra terms come from the contribution of the third-order microscopic hyperpolarizability. These extra contributions are a manifestation of local-field effects. We denote for convenience the direct contribution to the fifth-order susceptibility as

$$\chi_{\text{direct}}^{(5)} = N\gamma_{\text{at}}^{(5)}|L|^4L^2. \quad (37)$$

Similarly, the sum of the second and third terms on the left-hand side of Eq. (36c) (the cascaded contribution to $\chi^{(5)}$) can be denoted as

$$\chi_{\text{cascaded}}^{(5)} = \frac{12\pi}{10}N^2[2(\gamma_{\text{at}}^{(3)})^2|L|^4L^3 + |\gamma_{\text{at}}^{(3)}|^2|L|^6L]. \quad (38)$$

Then the total local-field-corrected $\chi^{(5)}$, which is the sum of the two contributions, can be written as

$$\chi^{(5)} = \chi_{\text{direct}}^{(5)} + \chi_{\text{cascaded}}^{(5)}. \quad (39)$$

As we pointed out in preceding sections of this paper, the result that we obtained for $\chi^{(5)}$ does not agree with that predicted by a straightforward generalization of the Bloembergen’s result given by Eq. (15). It is evident from Eqs. (15) and (36c) that the generalization (15) predicts the direct term only (the term proportional to $\gamma_{\text{at}}^{(5)}$) in the expression for the local-field-corrected $\chi^{(5)}$, and does not account for the cascaded contributions coming from the third-order microscopic hyperpolarizability. We have shown in this section that the cascaded terms arise from substituting the *nonlinear* local field into the expression (27b) for $P^{(3)}$. If we were limiting ourselves to considering the third-order nonlinearity (i.e., the lowest-order nonlinearity in our system), then we would need only to substitute the linear local field

$$E_{\text{loc}} = E + \frac{4\pi}{3}P^L,$$

into Eq. (27b) to deduce that

$$P^{(3)} = 3N\gamma_{\text{at}}^{(3)}|L|^2L|E|^2E,$$

instead of $P^{(3)}$ in the form of Eq. (33a). Thus, one clearly cannot simply use the generalization (15) to treat nonlinearity of the order higher than the lowest order of the nonlinearity present in the system of interest.

To develop insight into the relative contributions of the third- and fifth-order hyperpolarizabilities to the local-field-corrected fifth-order susceptibility (36c), we conduct a comparative analysis of the direct and cascaded terms. The analysis identifies the importance of the cascaded terms, and is presented in the following section.

III. NUMERICAL ANALYSIS

We perform our analysis based on a realistic example, taking the values of parameters for the sodium $3s \rightarrow 3p$ transition. The transition dipole moment is $|\mu| = 5.5 \times 10^{-18}$ esu and the population relaxation time is $T_1 = 16$ ns. The value of the coherence relaxation time T_2 can be found according to [6]

$$\gamma_2 = \frac{\gamma_{\text{nat}}}{2} + \gamma_{\text{self}}.$$

Here $\gamma_2 = 1/T_2$ is the atomic linewidth, $\gamma_{\text{nat}} = 1/T_1$ is the natural (radiative) linewidth, and the collisional contribution γ_{self} is given by

$$\gamma_{\text{self}} = \frac{4\pi N|\mu|^2}{\hbar} \sqrt{\frac{2J_g + 1}{2J_e + 1}},$$

where J_g and J_e are the angular momentum quantum numbers of the ground and excited states, respectively (for the sodium $3s \rightarrow 3p$ transition, $J_g = 0$ and $J_e = 1$).

In the theoretical analysis developed in the previous sections of this paper we have implicitly used the rotating wave approximation (RWA) to describe the atomic response. Before proceeding here we confirm the validity of that approximation for our example of the sodium $3s \rightarrow 3p$ transition. We begin by comparing our RWA expression (21) to a more precise expression in which the RWA approximation is not made,

$$\chi_{\text{non-RWA}}^{(1)} = \frac{N|\mu|^2}{\hbar} \left[\frac{1}{(\omega_{ba} - \omega + \Delta_L) - i/T_2} + \frac{1}{(\omega_{ba} + \omega - \Delta_L) + i/T_2} \right], \quad (40)$$

where it is the second term in Eq. (40) that is missing in the RWA. Evaluating $\text{Re}(\chi_{\text{non-RWA}}^{(1)})/\text{Re}(\chi^{(1)})$ and $\text{Im}(\chi_{\text{non-RWA}}^{(1)})/\text{Im}(\chi^{(1)})$ over the range of atomic densities and frequency detunings that we use in this section, we find that even at $N = 10^{17}$ cm⁻³ the maximum deviations of those ratios from unity are only a fraction of a percent. And even if the ratios are raised to the third and fifth powers, as a rough sense of how the higher order susceptibilities will be sensitive to expressions beyond the RWA, we find that their maximum deviations from unity are at most a few percent. Thus we feel comfortable in using the RWA in our identification of the range of validity of different approximations, and in our comparison of the contributions of the direct and cascaded fifth order terms.

Our goal is to identify the parameter space where the power-series expansion of the local-field-corrected susceptibility, including the total $\chi^{(5)}$ (36c), is valid. This defines what we call the “full fifth-order model.” Along the way it will be useful to also identify the ranges of validity of some other susceptibility models: (a) the local-field-corrected $\chi^{(1)}$, which is the expression for the total susceptibility neglecting the nonlinear interactions (we refer to this as the “linear model”); (b) the power-series expansion for the local-field-corrected total susceptibility given up to the third order of

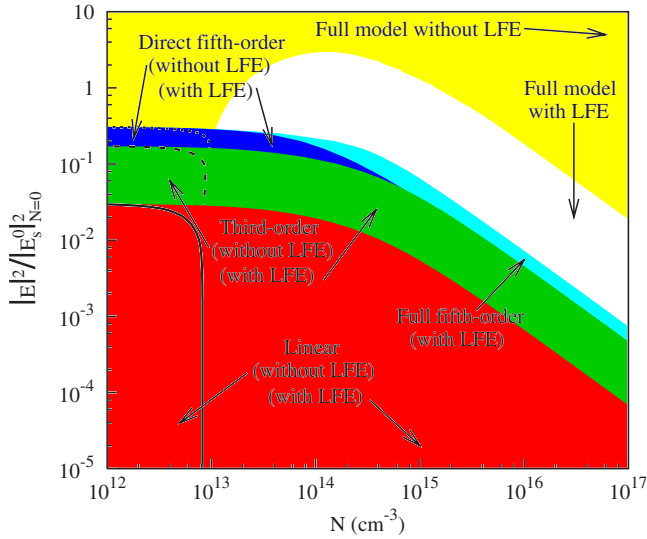


FIG. 1. (Color online) The ranges of validity of the various models described in the text for the total susceptibility of a collection of two-level atoms. The area at the bottom shows the range of validity of the linear model; local field effects (LFEs) are important in the region on the right but can be ignored on the left. Moving upward on the plot, the next area shows the range of validity of the third-order model. Again, LFEs can be ignored in the region on the left, and of course this model also accurately describes the response in the region below it. The next two regions show the ranges of validity of the direct fifth-order model and the full fifth-order model. In the white region above these colored regions, the full model of Eq. (42) must be used, and finally in the region at the top of the plot accurate predictions can be obtained by ignoring LFEs as long as the full model of Eq. (41) is used.

nonlinearity (we refer to this expansion as the “third-order model”); (c) the power-series expansion for the local-field-corrected total susceptibility given up to fifth order of nonlinearity neglecting the cascaded contribution (we refer to this as the “direct fifth-order model”); (d) the full expression for the susceptibility obtained without accounting for local-field effects, given as [17]

$$\chi = \frac{-N|\mu|^2 T_2}{\hbar} \frac{\Delta T_2 - i}{1 + \Delta^2 T_2^2 + |E|^2/|E_s^0|^2} \quad (41)$$

(we refer to this model as “full model without LFE”).

We identify the range of parameters over which the models are valid by comparing them to the full expression for the local-field-corrected total susceptibility

$$\chi = \frac{N|\mu|^2 T_2}{\hbar} \frac{w}{T_2(\Delta + \Delta_L w) + i}, \quad (42)$$

where the population inversion w is given by Eq. (8a) (we refer to this model as the “full model”). In order for a model to be valid for a given range of parameters (the atomic density and electric field strength), we require that at a given atomic density and normalized electric-field strength $|E|^2/|E_s^0|^2$ the difference between the full model and the other model at any detuning is not greater than 3% of the peak value of the full model. Using this criterion, the ranges over

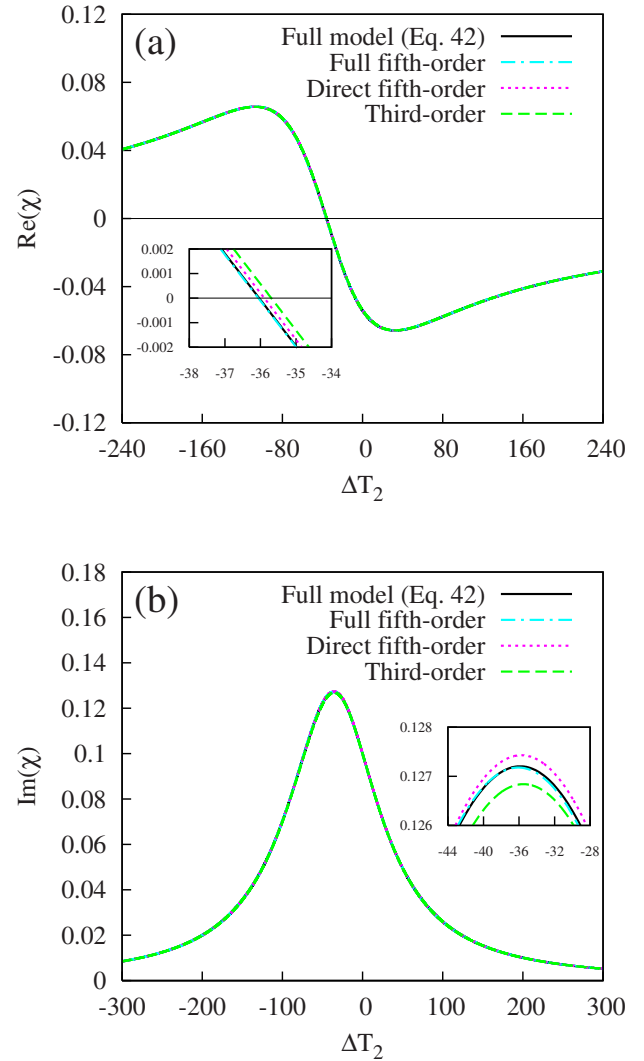


FIG. 2. (Color online) Real (a) and imaginary (b) parts of the total susceptibility of a collection of two-level atoms as functions of the detuning plotted for $N=10^{16} \text{ cm}^{-3}$ and $|E|^2/|E_s^0|^2=10^{-3}$. The susceptibility is given by different models, as depicted in the legend.

which the models are valid are marked with colored areas in Fig. 1. The full model without LFE can be used at higher strengths of the applied field where the saturation effect is strong, while at small values of the atomic densities the local-field effects are unimportant and one can neglect them in both the full model and the power series expansions.

Comparing the full fifth-order model to other power-series expansion models, we conclude that the former has a broader range of validity. As well, we find that the full fifth-order model gives a more precise description of the local-field-corrected susceptibility than the other power-series expansions in the ranges where all these models are valid. As an example, we plot the real and imaginary parts of the local-field-corrected susceptibility given by the different models as the function of the normalized frequency detuning ΔT_2 , where the value of T_2 is taken at zero atomic density, in Fig. 2. We see that for a given set of parameters all the power-series expansions describe the total susceptibility fairly well,

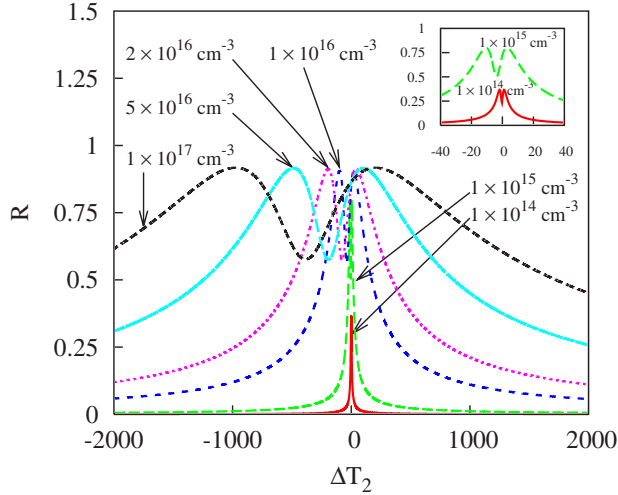


FIG. 3. (Color online) The ratio $R = |\chi_{\text{cascaded}}^{(5)}|/|\chi_{\text{direct}}^{(5)}|$ of the absolute values of the cascaded and direct contributions to the local-field-corrected $\chi^{(5)}$ as a function of the normalized detuning ΔT_2 plotted for several values of the atomic density falling into the range between 1×10^{14} and $1 \times 10^{17} \text{ cm}^{-3}$. The inset resolves the absolute values of the ratio for the atomic densities $N = 10^{14}$ and 10^{15} cm^{-3} .

but the inset reveals that the full fifth-order model works the best of all, as there is no apparent disagreement between it and the full model.

We now consider how the presence of the cascaded term affects the size and frequency dependence of $\chi^{(5)}$. In Fig. 3 we plot the ratio of the absolute values of the cascaded and direct terms as the function of the normalized detuning ΔT_2 for several values of the atomic density N within the range of 1×10^{14} to $1 \times 10^{17} \text{ cm}^{-3}$. We take the value of T_2 at $N=0$ in the normalized frequency detuning. It can be seen from Fig. 3 that the influence of the local-field effects is twofold. First, the local-field effects tend to shift the resonance feature towards lower frequencies by the amount Δ_L . The frequency shift grows linearly with the increase of the density N . Second, the ratio $|\chi_{\text{cascaded}}^{(5)}|/|\chi_{\text{direct}}^{(5)}|$ grows with increasing atomic density, as is especially clear from the inset in Fig. 3. This growth saturates at atomic densities higher than 10^{16} cm^{-3} , because homogeneous collisional broadening comes into play. Clearly, the cascaded term has a non-negligible contribution to the fifth-order susceptibility.

The result shown in Fig. 3, although informative, does not present a complete picture of the contribution to $\chi^{(5)}$ from the cascaded term. We can learn more by considering the real and imaginary parts of $\chi_{\text{direct}}^{(5)}$ and $\chi_{\text{cascaded}}^{(5)}$. These are plotted as functions of the normalized detuning ΔT_2 , where T_2 is taken at $N=0$, for different values of the atomic density in Figs. 4(a), 4(c), and 4(e). For the purpose of comparison, we also plot the total fifth-order susceptibility given by Eq. (39), which is the sum of the direct and cascaded contributions, and $\chi_{\text{direct}}^{(5)}$ [see Figs. 4(b), 4(d), and 4(f)]. The cascaded terms make an insignificant contribution until atomic densities reach on the order of 10^{13} – 10^{14} cm^{-3} [see Figs. 4(a) and 4(b)]. As the atomic density increases, the contribution from the cascaded term becomes more pronounced, as one can see

from Fig. 4(d). The difference becomes even more significant with further increase of the atomic density, and saturates at the densities higher than 10^{16} cm^{-3} .

Taking a careful look at the contribution to $\chi^{(5)}$ from the cascaded term [better seen in Fig. 4(f)], one can see not only a line shape distortion and a frequency shift of the maximum, but also a sign change of the imaginary part of $\chi^{(5)}$ in a certain range of detuning. This sign change, of course, cannot be observed in the total response of the two-level atom, since there is net absorption.

IV. CONCLUSION

We have performed a theoretical analysis of saturation effects in a dense medium using both the local-field-corrected Maxwell-Bloch equations and Bloembergen's approach. The expressions for the nonlinear susceptibilities, obtained using the two approaches, are in agreement. The equation obtained for the local-field-corrected fifth-order nonlinear susceptibility contains not only an obvious term coming from the fifth-order hyperpolarizability contribution (the direct term), but also two extra terms, proportional to the second power of the third-order hyperpolarizability. The two extra terms are induced purely by local-field effects. This kind of cascaded contribution from the lower-order hyperpolarizability to the higher-order nonlinear terms will appear in high-order susceptibilities describing other nonlinear effects as well.

We presented a comparative study of the direct contribution and the cascaded contribution to $\chi^{(5)}$ for the sodium $3s \rightarrow 3p$ transition. Our analysis shows that the relative contribution of the cascaded term to $\chi^{(5)}$ grows with the increase of the atomic density and saturates at atomic densities higher than 10^{16} cm^{-3} . At low atomic densities ($N < 1 \times 10^{14} \text{ cm}^{-3}$) the cascaded contribution to $\chi^{(5)}$ is insignificant. At high atomic densities ($N > 1 \times 10^{15} \text{ cm}^{-3}$) the value of the cascaded contribution is on the same order of magnitude as that of the direct contribution.

ACKNOWLEDGMENTS

We are grateful to Dr. S. N. Volkov for suggesting to address this problem using Bloembergen's approach. This work was supported by NSF Grant No. ECCS-0701585.

APPENDIX: MULTIPLE SOLUTIONS FOR THE POPULATION INVERSION

Let us consider in which part of parameter space Eq. (8a) has more than one physical solution. It is convenient to rewrite the equation in the form

$$w[1 + (\delta + \delta_L w)^2 + x] = -[1 + (\delta + \delta_L w)^2], \quad (\text{A1})$$

where $\delta = \Delta T_2$ is the detuning parameter, $\delta_L = \Delta_L T_2$ is the Lorentz redshift parameter, and $x = |E|^2/|E_s^0|^2$ is the electric field parameter. We rewrite Eq. (A1) as [36]

$$w^3 + a_2 w^2 + a_1 w + a_0 = 0, \quad (\text{A2})$$

where

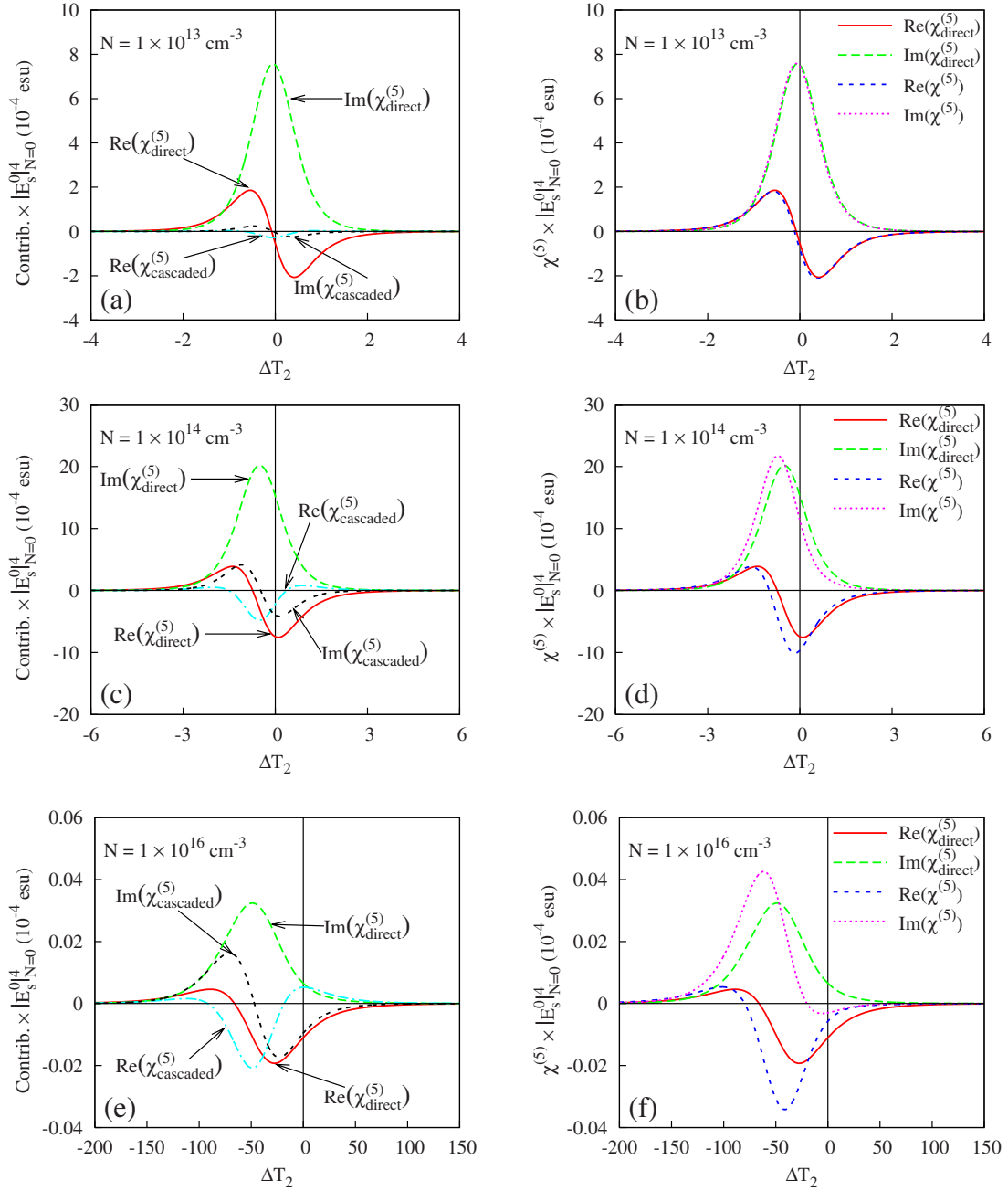


FIG. 4. (Color online) Real and imaginary parts of the direct and cascaded contributions to $\chi^{(5)}$, $\chi_{\text{direct}}^{(5)}$, and $\chi_{\text{cascaded}}^{(5)}$ (a), (c), (e) and the sum of the contributions $\chi_{\text{total}}^{(5)}$ plotted together with $\chi_{\text{direct}}^{(5)}$ (b), (d), (f) as functions of the normalized detuning for different values of the atomic density N .

$$a_0 = \frac{1 + \delta^2}{\delta_L^2}, \quad (\text{A3a})$$

$$q = \frac{a_1}{3} - \frac{a_2^2}{9} \quad (\text{A4a})$$

$$a_1 = \frac{1 + \delta^2 + x + 2\delta\delta_L}{\delta_L^2}, \quad (\text{A3b}) \quad \text{and}$$

and

$$a_2 = \frac{2\delta + \delta_L}{\delta_L}. \quad (\text{A3c})$$

$$r = \frac{a_1 a_2 - 3a_0}{6} - \frac{a_2^3}{27}, \quad (\text{A4b})$$

Then, constructing

we look at the sign of the parameter

$$D = q^3 + r^2. \quad (\text{A5})$$

If $D > 0$, there is one real root and a pair of complex conjugate roots; if $D = 0$ all roots are real and at least two are equal; if $D < 0$ all three roots are real (irreducible case) [36]. In order to achieve multiple physical solutions, we need the values of w to be real (and in the range -1 to $+1$). Certainly a necessary condition for this is $D \leq 0$. Introducing

$$s_1 = [r + (q^3 + r^2)^{1/2}]^{1/3} \quad (\text{A6a})$$

and

$$s_2 = [r - (q^3 + r^2)^{1/2}]^{1/3}, \quad (\text{A6b})$$

we write the solutions to Eq. (A2) in the form [36]

$$w_1 = (s_1 + s_2) - \frac{a_2}{3}, \quad (\text{A7a})$$

$$w_2 = -\frac{1}{2}(s_1 + s_2) - \frac{a_2}{3} + \frac{i\sqrt{3}}{2}(s_1 - s_2), \quad (\text{A7b})$$

and

$$w_3 = -\frac{1}{2}(s_1 + s_2) - \frac{a_2}{3} - \frac{i\sqrt{3}}{2}(s_1 - s_2). \quad (\text{A7c})$$

We now consider certain fixed values of the redshift parameter δ_L , and investigate the ranges of δ and x for which multiple physical solutions exist. Such ranges are marked with contours on the graphs in Fig. 5. For the values of parameters δ and x lying inside the contours there are three physical solutions to Eq. (A2) with the corresponding values of w being within the range $[-1, 1]$. The area outside the

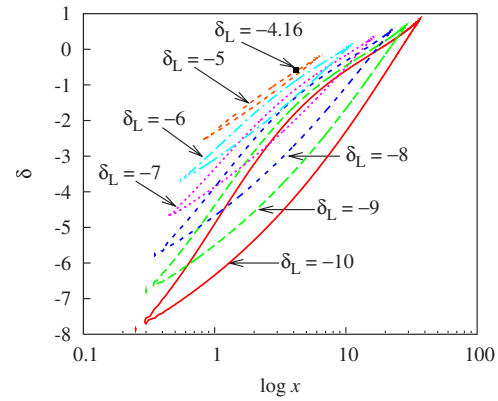


FIG. 5. (Color online) The ranges of values of the detuning parameter δ and the electric field parameter x for which mirrorless optical bistability is achievable (marked with contours). Different contours correspond to different values of the Lorentz redshift parameter δ_L . The point corresponds to the limiting value $\delta_L = -4.16$: for $|\delta_L| < 4.16$ there are no ranges of δ and x at which optical bistability is achievable.

contours corresponds to a single physical solution for w , with the other two solutions being complex and, therefore, non-physical. According to our numerical analysis, summarized in Fig. 5, multiple physical solutions only arise for $|\delta_L| \geq 4.16$. In sodium vapor that we consider as an example for our analysis in Sec. VI, such large values of δ_L are not achievable; raising the density to increase Δ_L also decreases T_2 due to homogeneous broadening, and δ_L can never get this large.

[1] J. Guo, J. Cooper, and A. Gallagher, Phys. Rev. A **53**, 1130 (1996).
 [2] F. A. Hopf, C. M. Bowden, and W. H. Louisell, Phys. Rev. A **29**, 2591 (1984).
 [3] I. Abram and A. Maruani, Phys. Rev. B **26**, 4759 (1982).
 [4] F. A. Hopf and C. M. Bowden, Phys. Rev. A **32**, 268 (1985).
 [5] Y. Ben-Aryeh, C. M. Bowden, and J. C. Englund, Phys. Rev. A **34**, 3917 (1986).
 [6] J. J. Maki, M. S. Malcuit, J. E. Sipe, and R. W. Boyd, Phys. Rev. Lett. **67**, 972 (1991).
 [7] H. van Kampen, V. A. Sautenkov, C. J. C. Smeets, E. R. Eliel, and J. P. Woerdman, Phys. Rev. A **59**, 271 (1999).
 [8] C. R. Stroud, Jr., C. M. Bowden, and L. Allen, Opt. Commun. **67**, 387 (1988).
 [9] N. Wang and H. Rabitz, Phys. Rev. A **51**, 5029 (1995).
 [10] J. P. Dowling and C. M. Bowden, Phys. Rev. Lett. **70**, 1421 (1993).
 [11] A. S. Manka, J. P. Dowling, C. M. Bowden, and M. Fleischauer, Phys. Rev. Lett. **73**, 1789 (1994).
 [12] A. S. Manka, J. P. Dowling, C. M. Bowden, and M. Fleischauer, Quantum Opt. **6**, 371 (1994).
 [13] S. Singh, C. M. Bowden, and J. Rai, Opt. Commun. **135**, 93 (1997).
 [14] A. S. Zibrov, M. D. Lukin, L. Hollberg, D. E. Nikonov, M. O. Scully, H. G. Robinson, and V. L. Velichansky, Phys. Rev. Lett. **76**, 3935 (1996).
 [15] A. S. Zibrov, A. B. Matsko, L. Hollberg, and V. L. Velichansky, J. Mod. Opt. **49**, 359 (2002).
 [16] N. Bloembergen, *Nonlinear Optics*, 4th ed. (World Scientific, Singapore, 1996).
 [17] R. W. Boyd, *Nonlinear Optics*, 2nd ed. (Academic Press, New York, 2003).
 [18] Y. R. Shen, *The Principles of Nonlinear Optics* (Wiley, New York, 1984).
 [19] E. Yablonovitch, C. Flytzanis, and N. Bloembergen, Phys. Rev. Lett. **29**, 865 (1972).
 [20] S. D. Kramer, F. G. Parsons, and N. Bloembergen, Phys. Rev. B **9**, 1853 (1974).
 [21] G. R. Meredith, Phys. Rev. B **24**, 5522 (1981).
 [22] R. DeSalvo, D. J. Hagan, M. Sheik-Bahae, G. Stegeman, E. W. Van Stryland, and H. Vanherzeele, Opt. Lett. **17**, 28 (1992).
 [23] G. I. Stegeman, M. Sheik-Bahae, E. Van Stryland, and G. Asanto, Opt. Lett. **18**, 13 (1993).
 [24] Y. Baek, R. Schiek, and G. I. Stegeman, Opt. Lett. **20**, 2168 (1995).
 [25] R. Schiek, Y. Baek, and G. I. Stegeman, Phys. Rev. E **53**, 1138

- (1996).
- [26] J. B. Khurgin, A. Obeidat, S. J. Lee, and Y. J. Ding, *J. Opt. Soc. Am. B* **14**, 1977 (1997).
- [27] G. I. Stegeman, D. J. Hagan, and L. Torner, *Opt. Quantum Electron.* **28**, 1691 (2004).
- [28] G. I. Stegeman, *Quantum Semiclassic. Opt.* **9**, 139 (1997).
- [29] D. Bedeaux and N. Bloembergen, *Physica (Amsterdam)* **69**, 57 (1973).
- [30] J. Ducuing, in *Nonlinear Optics*, edited by P. G. Harper and B. S. Wewrrett (Academic Press, New York, 1975).
- [31] C. Flytzanis, in *Quantum Electronics*, edited by H. Rabin and C. L. Tang (Academic Press, New York, 1975).
- [32] G. R. Meredith, in *Nonlinear Optics: Methods and Devices*, edited by C. Flytzanis and J. L. Oudar (Springer-Verlag, Berlin, 1986).
- [33] J. H. Andrews, K. L. Kowalski, and K. D. Singer, *Phys. Rev. A* **46**, 4172 (1992).
- [34] C. Kelleck, *Phys. Rev. A* **69**, 053812 (2004).
- [35] H. A. Lorentz, *Theory of Electrons*, 2nd ed. (Teubner, Leipzig, 1916).
- [36] M. Abramowitz and I. A. Stegun, *Handbook of Mathematical Functions with Formulas, Graphs, and Mathematical Tables*, 10th printing (National Bureau of Standards, Washington, D.C., 1972).